ГЕОМОРФОЛОГИЯ, 2022, том 53, № 5, с. 32–47

ПРОБЛЕМЫ ПАЛЕОПОЧВОВЕДЕНИЯ И ГЕОАРХЕОЛОГИИ

УДК 551.89:574→631.42:902/904 (470.323)

РЕКОНСТРУКЦИЯ ПАЛЕОЛАНДШАФТОВ СРЕДНИХ ВЕКОВ НА ОСНОВЕ ИЗУЧЕНИЯ ПОГРЕБЕННЫХ ПОЧВ ГОЧЕВСКОГО АРХЕОЛОГИЧЕСКОГО КОМПЛЕКСА (КУРСКАЯ ОБЛАСТЬ)

© 2022 г. Ф. Г. Курбанова[1,*], Т. А. Пузанова[2], Е. Н. Асеева[2], П. Г. Куст[3], О. В. Руденко[4]

[1]Институт географии РАН, Москва, Россия

[2]Московский государственный университет имени М.В. Ломоносова, географический факультет, Москва, Россия

[3]Почвенный институт имени В.В. Докучаева, Москва, Россия

[4]Орловский государственный университет имени И.С. Тургенева, Орел, Россия

*****E-mail: fatima.kurbanova@igras.ru*

Поступила в редакцию 14.06.2022 г.
После доработки 20.06.2022 г.
Принята к публикации 15.07.2022 г.

Благодаря изолированности от внешней среды, почвы, погребенные под курганными могильниками, являются ценными архивами, которые содержат информацию о природных условиях прошлых эпох. Приведены результаты изучения почв, погребенных под курганами в средневековье с небольшим временным интервалом – 25–50 лет. В исследования входили подробное полевое морфологическое описание почв, гранулометрический анализ, изучение элементного состава, фракционного железа и некоторых других физико-химических параметров. Помимо этого, был выполнен анализ спор, пыльцевых и непыльцевых палиноморф. Для сравнения была исследована фоновая почва в непосредственной близости от курганов. Полученные данные позволили определить динамику лесостепных ландшафтов в X–XI вв. Произошедшие в этот временной отрезок средневековое потепление и последующее увлажнение климата за короткий период могли существенно повлиять на природные условия и миграцию населения степей Евразии.

Ключевые слова: палеопочвы, спорово-пыльцевой анализ, палеоклимат, голоцен, средневековый климатический оптимум

DOI: 10.31857/S0435428122050078

1. INTRODUCTION

Soils buried under burial mounds are one of the natural archives that can store information on the natural conditions of the past. Due to isolation from the external environment, "conservation" occurs. As a result, the profile of the buried soil can preserve some signs that retain information about the features of the natural environment at the time of its burial.

A comparative analysis of the properties of soils buried under archaeological sites of different ages allows a detailed study of the changes in the natural environment and its components over time. In addition, soils can store a whole range of additional features of non-pedogenic origin, which can be used for a more detailed reconstruction of the natural environment. Thus, spores and pollen of plants, phytoliths, faunal remains, etc., are preserved in the soil profile. Therefore, the soil profile can be considered a kind of data archive containing unique information about the features of past natural settings.

Currently, the climatic changes during the Medieval Climate Optimum and the Little Ice Age within the forest-steppe of Central Russia have been poorly understood. According to accepted chronology, a Medieval Climate Anomaly corresponds to the 8th–13th centuries AD (Klimenko et al., 2001; Goosse et al., 2012). This period was characterised by sharp warming of the climate for most of the northern hemisphere. The warming peak was noted for the chrono-interval of the 10th–11th centuries AD. The analysis of Russian chronicles indicated that the climate of the European part of Russia changed significantly during this time (Borisenkov et al., 1983). In some periods, during extreme natural phenomena such as droughts, climate change led not only to the famine of population but also to social upheaval. According to the chronicles, the climate of ancient Russia during the period of the Medieval Climate Optimum in the 9th and 11th centuries was characterised by frequent droughts. From the 12th century, Russian chronicles indicate an increase in intra-seasonal and extreme climate variability and a shift to long cold winters, rainy weather in the

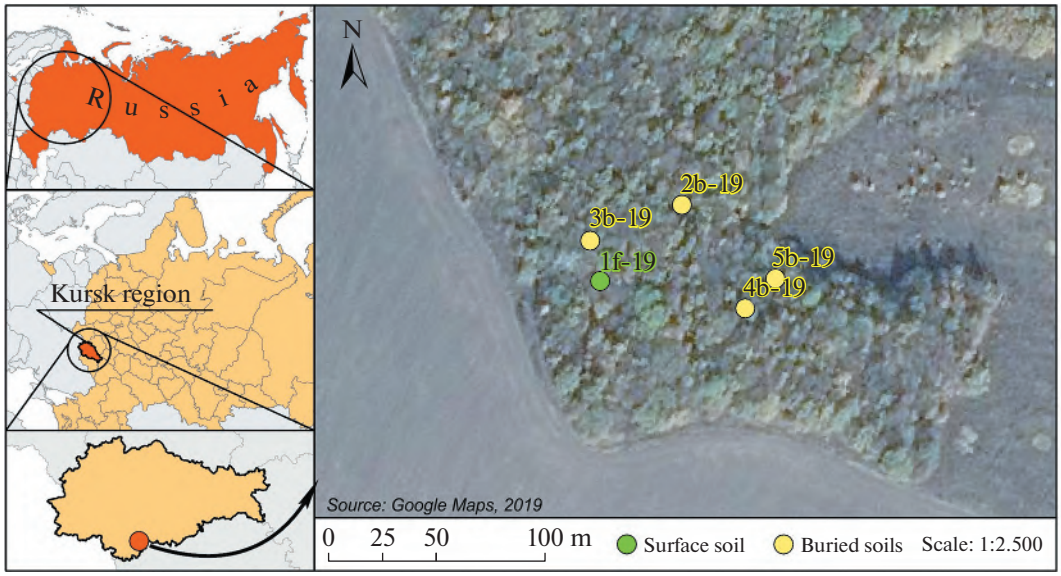

Fig. 1. Location of the study area (Kurbanova et al., 2020).
Рис. 1. Местоположение территории исследования (Kurbanova et al., 2020).

summer seasons, early frost in late summer and early fall. All these weather phenomena were the precursors of the Little Ice Age. The first third of the 12th century is considered the transition to the Little Ice Age. At this time, the number of floods and summer early frosts increased, which led to the death of crops and was the cause of hunger, epidemics and population fall (Borisenkov et al., 1983).

However, during medieval climate warming and cooling periods, there were significant decadal and secular temperature fluctuations. So, on the territory of the Russian Plain, the warmest over the past 2000 years was the 10th century, after which there was a clear trend towards a cooling of the climate. The Medieval Climate Optimum, which began about 1100 years ago, was characterised by the average annual temperature and by higher humidity. Precipitation during this period was ~25–50 mm more than nowadays (Kupriyanova et al., 1972).

We studied the surface soils and the soils buried under four mounds of the Gochevsky archaeological complex, located in the Kursk region, Russia. All mounds were constructed during the 11th century, with time intervals ranging from 25 to 50 years, enabling one to provide a detailed reconstruction of paleolandscapes for the 11th century. Our study aimed to evaluate the transformation of various properties of the soils in the forest-steppe zone over 25–50 years based on the study of a short-time soil series formed under similar lithological and topographic conditions using a single set of soil and biomorphic methods. This approach has already been used in several studies. In particular, O.S. Khokhlova (2016) compared soils under mounds with a difference in burial time of 25–50 years in the steppe zone.

2. STUDY AREA

The Gochevsky archaeological complex is located on the right bank of the river Psel near settlement Gochevo in Belovsky district (Kursk region, Russian Federation) within the Central Russian forest-steppe province of the East European Plain (fig. 1). The Gochevsky burial ground is one of the largest identified and survived monuments in modern Eastern Europe. The entire burial ground consisted of three thousand burial mounds; however, after intensive ploughing, only sites under the forest survived. In total, about 800 mounds were preserved in a small area currently occupied by deciduous forests. Gochevsky burial ground contains funeral rites of the old Russian population of the southeast of Russia at the end of the 10–12 centuries AD. All soil pits are located in the watershed area.

The climate of the study area is temperate continental, with moderately cold winters and warm summers. The average annual air temperature is about +7°C. Mean annual precipitation ranges from 475 to 640 mm. The warm period (April-October) accounts for 65–70% of the annual precipitation. Permanent snow cover is established in the second ten days of December; in early March, snowmelt begins, lasting about 20 days. The height of the snow cover ranges from 15 to 30 cm (maximum 50 cm) and persists on average for 2–2.5 months.

The natural steppe vegetation, typical of the forest-steppe zone, is preserved in the Central Chernozem Nature Reserve. It occurs only on slopes of gullies in

the study area since the entire area has been almost completely ploughed. The forest vegetation covers less than 10% of the study area. It is represented mainly by oak forests and also by forest shelterbelts.

Quaternary loess deposits serve as parent material for soil formation. At depth, loess is underlain by Paleogene and Neogene sands and argillaceous deposits. The dominant soil type in the study area is chernozem (75%); dark grey forest soils occur under broad-leaved forests. Due to ploughing, the soils are highly eroded.

3. MATERIAL AND METHODS

Research objects. Soils buried under four mounds with a thickness of 40–60 cm were examined. The soils were formed in the same topographic position, in the interfluve area covered by forest vegetation and in the similar parent material. Their soil profiles were considered as a data archive containing information on the past environments. The soils 3b, 4b, 5b were buried over the period from the second quarter to the middle of the 11th century, while the soil 2b was buried later, in the second half of the 11th century. Burial mounds were dated by archaeological method (Puzanova et al., 2018). To compare the conditions of the past to the modern ones, the surface soil (1f) formed in the was also studied. All buried and surface soils were located under one forest patch at a distance of 25–100 meters from each other.

Sampling and laboratory analyses. Samples were collected from the buried soils below the burial mound from every 10 cm down to 1 m (and every 20 cm below 1 m) but with the preservation of the soil horizon intact. Samples of soils for pollen analysis were taken from the upper 0–5 cm of the buried and the surface soils. The soils were described according to the FAO Guidelines for Soil Description (2006). Soil colour was determined in the field using the Munsell Soil Color Charts (2014).

Two methods to determine particle size distribution in soil horizons were used: pipette method, in which soil was dispersed by treating with a solution of sodium pyrophosphate ($Na_4P_6O_{18}$) and laser granulometry method using FRITSCH laser particle sizer Analysette 22. Laser Klasse 1 (Germany). The boundaries between particle size classes were defined by the Russian conventional fraction groups: the coarse and medium sand fraction (1–0.25 mm); the fine sand fraction (0.25–0.05 mm); the coarse (0.05–0.01 mm), the medium (0.005–0.001 mm), the fine silt (0.005–0.001 mm) and the clay fraction (<0.001 mm). Textural classes were approximated according to the FAO Guidelines for soil description (2006).

Dithionite and oxalate extractable fractions of iron were determined according to Mehra and Jackson (1960) using Cary 60 Spectrophotometer (Agilent Technologies, Santa Clara, CA, USA). The elemental analysis was performed by X-ray fluorescence spectrometry method after a loss on ignition determination (1000°C) using the Philips PW2400 Sequential WXRF Spectrometer (Malvern Panalytical, Almelo, The Netherlands). In sample preparation for the XRF analysis, ~1 g of sample was dried in the oven at 105°C. Samples were powdered, mixed with a lithium tetraborate flux and then melted to produce a glass disc.

The elemental data treatment included the calculation of the ratios of immobile elements – Ti, Al, Nb and Zr – which were used to evaluate the parent material uniformity (Sheldon et al., 2009). The amount of loss and gain in soil horizons relative to the parent material was quantitatively assessed using the eluvial/illuvial coefficient, or EIC [EIC(%) = $= ((Xh/Ih)/(Xr/Ir) - 1) \times 100\%$ (1), where X*h* and X*r* are the contents of element X, while I*h* and I*r* are the contents of an immobile element (Al) in soil horizons and parent rocks, respectively. Positive *EIC* values mean that the element has been enriched in the soil horizon and a negative value indicates the loss of the element. Eluvial-illuvial coefficients were estimated for relatively mobile elements, such as Ca, Sr, and also for Fe.

Micromorphological features of the thin sections made from undisturbed oriented samples were studied in plain (PPL) and polarized (XPL) light under 40 to 200 times magnification using an Olympus BX51 polarizing microscope. Olympus StreamBasic software was used for image capturing. In total 36 thin sections were described based on the terminology of Stoops (2003), with special attention on the variability of humus content, carbonate and clay pedofeatures. The work was carried out using the equipment of the Collective Centre "Functions and properties of soils and soil cover" of the V.V. Dokuchaev Soil Science Institute RAS.

For the extraction of microfossils, centrifugal separation in potassium-cadmium ($KJ + CdJ_2$) heavy liquid with a density of 2.3 g/cm^3 was used. Prior to this, samples were processed with cold 10-% solution of HCl and 10-% solution of KOH to dissolve carbonates and then decanted with distilled water to remove clay particles. Samples were stored in glycerin and examined under 400× magnification. Pollen identification and taxonomy follows Beug (2004), Kupriyanova and Aleshina (1972) and electronic databases of photos (http://www.europeanpollendatabase.net/index.php; https://www.paldat.org/) as well. Organic residues of aquatic microorganisms, spores of coprophilous and parasitic fungi on decaying plants and roots, indefinable spores of fungi were grouped as non-pollen palynomorphs (NPP), counted in addition and identified following NPP database (Shumilovskikh et al., 2021). In each sample, the number of micro-charcoal particles, which are among the effective eco-indicators, was also counted. Both pollen and NPP diagrams were constructed using Tilia 2.0.2 and TGView software

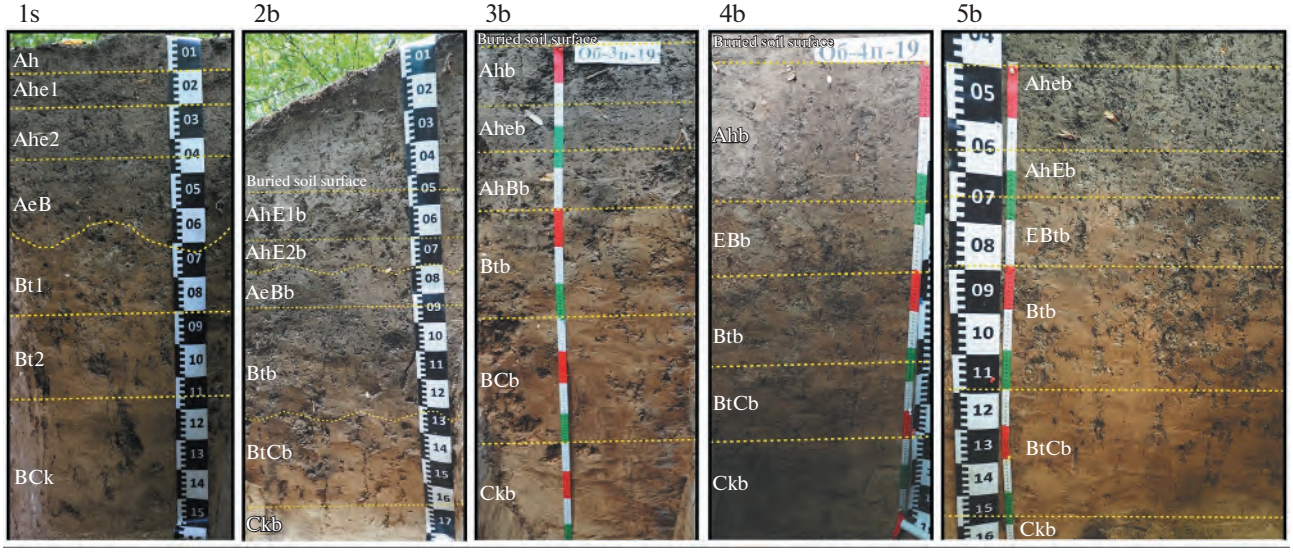

Fig. 2. Profiles of buried and surface soils.
Рис. 2. Профили погребенных и фоновой почв.

(Grimm, 1991). Calculation of pollen percentages was based on the terrestrial pollen sum – arboreal pollen (AP) plus non-arboreal pollen (NAP) without aquatic plants, spores and NPP. Their percentages were calculated based on AP+NAP sum.

4. RESULTS AND DISCUSSION

4.1. Soil morphology. All soils were formed in loess sediments and were classified as Greyzemic Luvic Phaeozem Cutanic. Uncoated silt and sand grains on the ped faces in the lower part of a humic horizon (AhE) indicate Greyzemic features (IUSS WRB Working group, 2015). The argic horizon is characterised by angular blocky/prismatic structure and clay cutans on the ped surfaces. Soils differed by the colour of humus horizon, amount and forms of carbonates, and intensity of greyzemic features.

The surface soil (1s) is represented by the following horizons: Ah-Ahe1-Ahe2-AeB-Bt1-Bt2- BCk (fig. 2-1s). The Ah horizon is characterised by granular structure and brownish-grey colour (7.5 YR 4–5/1). The next two horizons have subangular blocky and platy structures and contain uncoated quartz and feldspar grains on ped surfaces. Transitional AeB horizon, as well as Bt horizon, have an angular blocky structure with grey siltans (7.5 YR 7/1) and dark brownish-black cutans (5 YR 3/2). Bt2 horizon is characterised by prismatic structure and darker colour of cutans covering all transhorizontal cracks. The lowermost horizon BCk is distinguished by dull yellowish-orange colour (10 YR 6/4) and the presence of carbonates occurring as soft nodules and tiny tubules.

The thickness of the mound under buried soil 2b is 55 cm. The mound consists of dark grey material with abundant siltanes on angular blocky peds. The surface of the buried soil is determined by the darker colour of the humus horizon. The soil consists of the following horizons: AhE1b- AhE2b- AeBb- Btb- BtCb-Ckb (fig. 2–2b). The AhE1b horizon is grey/dark grey (10 YR 5–4/1) with abundant siltans. The second horizon has a darker colour (10 YR 3/1 very dark grey) and also contains uncoated sand and silt grains on the peds surfaces. In the AeBb the siltans are less distinct, and thin rare clay cutans appear. The structure in the Btb horizon is angular blocky, and prismatic; siltans are still present, but less common. At a depth of 110 cm, the Ckb horizon begins. It has a weak structure and contains carbonates presented as plasma and small dull yellowish-orange (10 YR 6/4) tubules.

The paleosoil 3b consists of the following horizons: Ahb- Aheb- AhBb- Btb- BCb-Ckb. The distinctive feature of this soil is the dark colour of the Aheb horizon (10YR 2/1). Greyzemic features are less intensive in this soil compared to other buried and surface soils (fig. 2–3b). The subsoil contains a high amount of dark cutans and is characterised by moderate angular blocky and prismatic structure. The deepest Ckb horizon has rounded ooids with brownish colour and carbonates in the form of small tubules that also occur in other soils from the archaeological complex.

The buried soils 4b and 5b (fig. 2–4b, 5b) have similar morphological characteristics. The following horizons represent the soil profiles: Ahb-EBb-Btb-BCb-Ckb (4b), and Aheb-AhEb-EBtb-BtCb-Ckb (5b). The upper horizons in both soils are characterised by dark grey colour (10 YR 3/1) and have a subangular blocky structure. Uncoated quartz and feldspar grains are frequent in the EBb (4b soil) and EBtb (5b soil) horizons. The Bt horizons have a prismatic structure

and contain clay-humus cutans. The transitional BCb horizons are not homogeneous in colour: they have a yellowish-brown colour of the soil matrix and a dark yellowish-brown (10 YR 4/4) colour of the coatings. The Ckb horizons were distinguished by weak structure and very pale brown colour with rounded brown ooids.

Although all soils were formed in loess deposits and were classified as *Folic Greyzemic Luvic Phaeozem Cutanic*, they differed in the colour of humus horizons and the deepness of the uncoated sand and silt grains occurrence. The soil 3b had a darker colour of the humus horizon (10YR 2/1) than other soils of the archaeological complex (10YR 3/1). The depth where uncoated sand and silt grains still occurred was also different; in the surface soil, they reached the depth of 90 cm; in the soil 2b, they could be traced up to 80 cm; in other soils uncoated sand and silt grains penetrated not deeper than 70 cm. In all the studied soils, the cutan complex was equally well expressed; however, humus cutans across transhorizontal cracks were found only in the surface soil.

4.2. Particle size distribution. All studied soils are characterised by silty loam texture. The dominant particle size fraction in the soil material in all five soil profiles is the coarse silt (fig. 3) because the soils are developed in loess deposits that formed during the Late Pleistocene cold periods. The amount of this particle size fraction varies between 40 and 61%. The surface soil 1f and the buried soils 2b and 3b contain nearly equal average amounts of the coarse silt particles (52–53%). However, its share in the buried soils 4b and 5b is slightly higher (55–56%). The sand is dominated by the fine sand fraction (0.25–0.05 mm). All soils don't differ significantly according to their average amount (4–5%) except the buried soil 2b containing a lower proportion of the sand-sized material. The vertical distribution of the sand particles follows different patterns in the studied soils. Distinct accumulation of the fine sand was recorded in the surface soil in its upper horizons, but in soil 2b the middle horizons contain more sand than other horizons, and in the soil profiles 4b and 5b the sand tends to accumulate in the BC or C horizons. The enrichment of the uppermost horizons with sand particles might be due to losses of finer material with infiltrating water, while the accumulation in the lower strata can be due to the effect of underlying sandy lithology. The vertical distribution of the clay in different soil profiles does not imply strong textural contrast between their upper and middle (Bt) horizons. In the surface soil, the clay fraction displays depletion in the topsoil and a relative increase in the lowermost parent material, where the clay content reaches its maximum (14%). No notable enrichment in the clay-sized material is registered in the Bt horizon. In the buried soils 2b, 3b and 4b, the changes are very smooth: the ratio of the clay contents in the AhEb and Bt horizons does not exceed 1.1 and the clay size particles tend to enrich subsoil.

In contrast to these soils, soil profile 5b shows a maximum clay content in the middle horizons. The estimated ratio for the AhEb and BtC horizons varies between 1.2–1.4. Thus, the clay fraction distribution in most soil profiles is rather uniform except for the surface soil and the buried soil 5b.

4.3. Soil micromorphology. At the microscale, a differentiation of humus horizons by colour is visible. Buried soils 2b, 4b, 5b show microzonality with low contrast between the light and dark microzones characterised by different amounts of humus (fig. 4, (c-f)). This contrast increases in the soil 1s mostly because of the darker humus microzones than in the soils 2b, 4b, 5b (fig. 4, (g, h)). In soil 3b, the humus horizon is homogeneous and has a darker colour compared to the other studied profiles (fig. 4, (a, b)).

The described features point out: 1) the stability of humus material at the moment of the soil 3b; 2) weak degradation of humus at the moment of soils 2b, 4b, 5b burial and a relatively higher degree of humus material degradation at present. The latter can be caused by a higher amount of precipitation described for the modern environment (Makeev et al., 2020).

Weak signs of humus horizon degradation in soil 3b correspond to the weakly developed complex of coatings in this profile (fig. 5, (a, b)). In the other buried soils, the degradation of the humus horizon is accompanied by the expression of clay coatings (fig. 5, (c–e)) and coatings of clear silt grains. In soils, 4b, 5b, abundant silty coatings are represented by lighter elongated zones around the aggregates (fig. 4, (c, d)). In the 2b soil profile, abundant well-defined silty coatings correlate with the better developed two-layered complex coatings. Such coatings consist of a clay layer (typical for all profiles) and a layer of dark clay-humus coatings (fig. 5, (e, f)) which are described only in 2b and surface soils. Abundant clay coatings increase in soils as follows: 3b – 4b, 5b – 2b – 1s (fig. 6, (a–d)).

Clay coatings are well expressed in all studied soils up to the depth of 100–120 cm. In the lower horizons, they are superimposed and overlap carbonate pedofeatures which are typical in lower horizons in all soils and especially in soil 3b (fig. 6, (e)). The carbonate pedofeatures are represented by micritic coatings. However, in the 3b profile, sparite nodules, which are typical for a more arid environment (National Soil Atlas..., 2011), were also detected (fig. 6, (f)). Carbonate and clay coatings interlayer suggests that the carbonate coatings have been formed first, and clay coatings started to form after them, but before the burial of 3b soil. Later, clay coatings were only slightly transformed, increasing their thickness at the further stages of evolution (2b – 1s), reflecting the changes in the paleoenvironment.

All studied soils save features of the previous stages of soil formation with palimpsests type of soil memory (Soil memory, 2008). Thus, earlier arid features are a) carbonate material in the lower layer of complex coat-

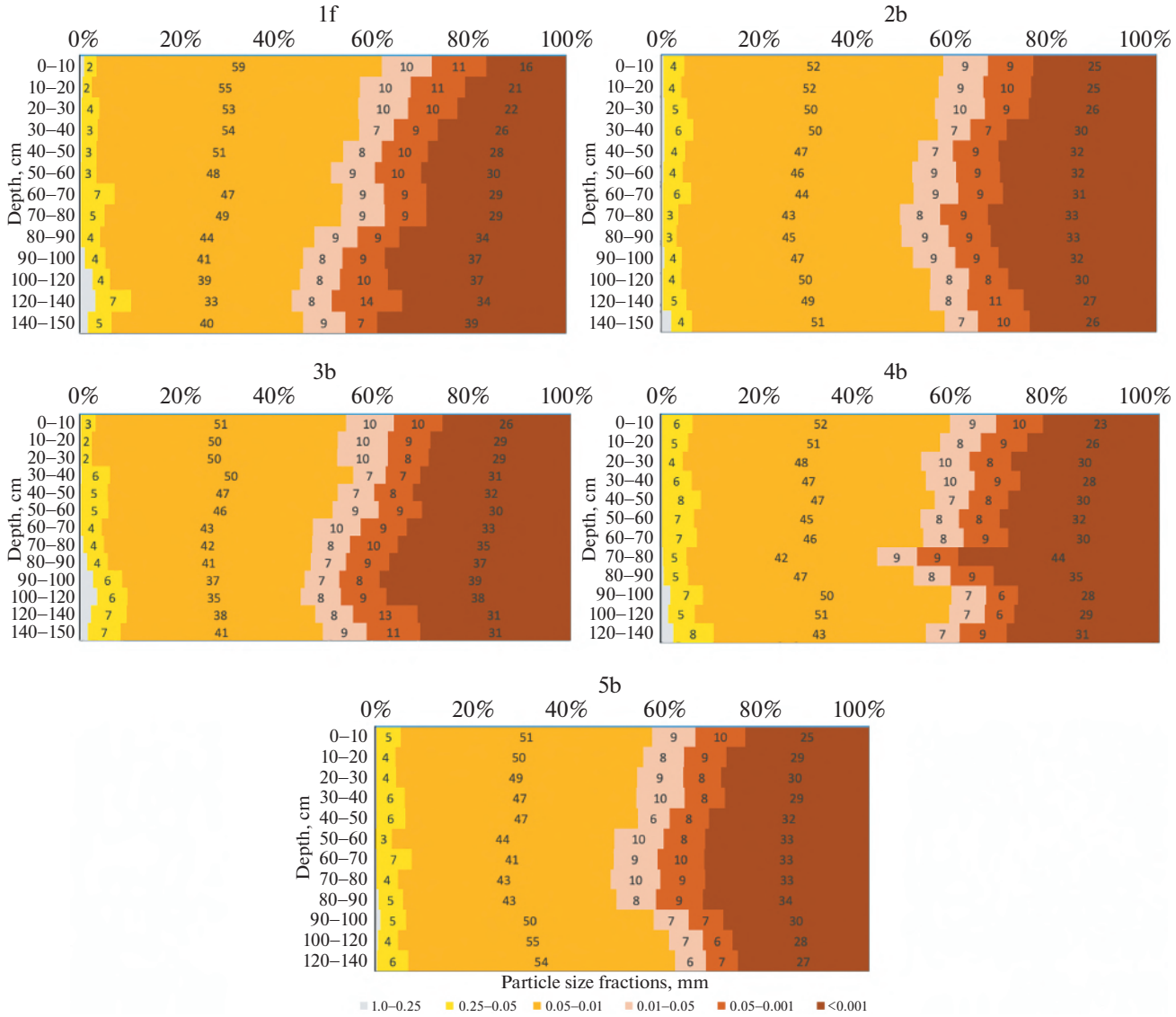

Fig. 3. Particle size distribution, with depth, in the surface soil 1s and the buried soils 2b, 3b, 4b and 5b.
Рис. 3. Гранулометрический состав почв в фоновой почве 1s и погребенных почвах 2b, 3b, 4b, 5b.

ings, b) dark humus horizons or microzones; later humid features are: a) silty coatings in the humus horizons, b) upper clay layers in complex coatings.

Fe-Mn pedofeatures were also described at the microscale in the studied soils. However, we can use them only as an additional indicator of soil-forming conditions since they are very alterable in time. Nevertheless, they are almost absent in the 3b profile (fig. 4, (a, b)), higher amounts – in the 4b and 5b profiles (fig. 4, (c, d)), the maximum amount was described in soils 2b, 1s (fig. 4, (e, f)).

4.4. Elemental analysis. The elements Ti, Zr and Nb are presumably not lost due to weathering and translocation (Sheldon et al, 2009, Muir et al., 1982, Schaetzl et al., 2005), and Al which is also inert under semi-humid climatic conditions, were chosen for the detection of lithogenic discontinuities. The ratios of these elements calculated for the soils' parent materials are nearly equal (tabl. 1), indicating that the sediments had been very likely derived from the same source. Additionally, the values calculated for soil horizons in each soil profile display very low variations (in most cases less than 10%), which means that lithogenic discontinuities are not present and the soil strata at each site are relatively homogeneous in terms of parent material origin and its mineralogical composition (Marsan et al., 1988). Taking into account these facts, it is possible to relate the pedogenic differences between the buried and surface soils to environmental changes that occurred after the burial.

In all five studied soils, the eluvial-illuvial coefficients calculated for Ca and Sr had negative values in

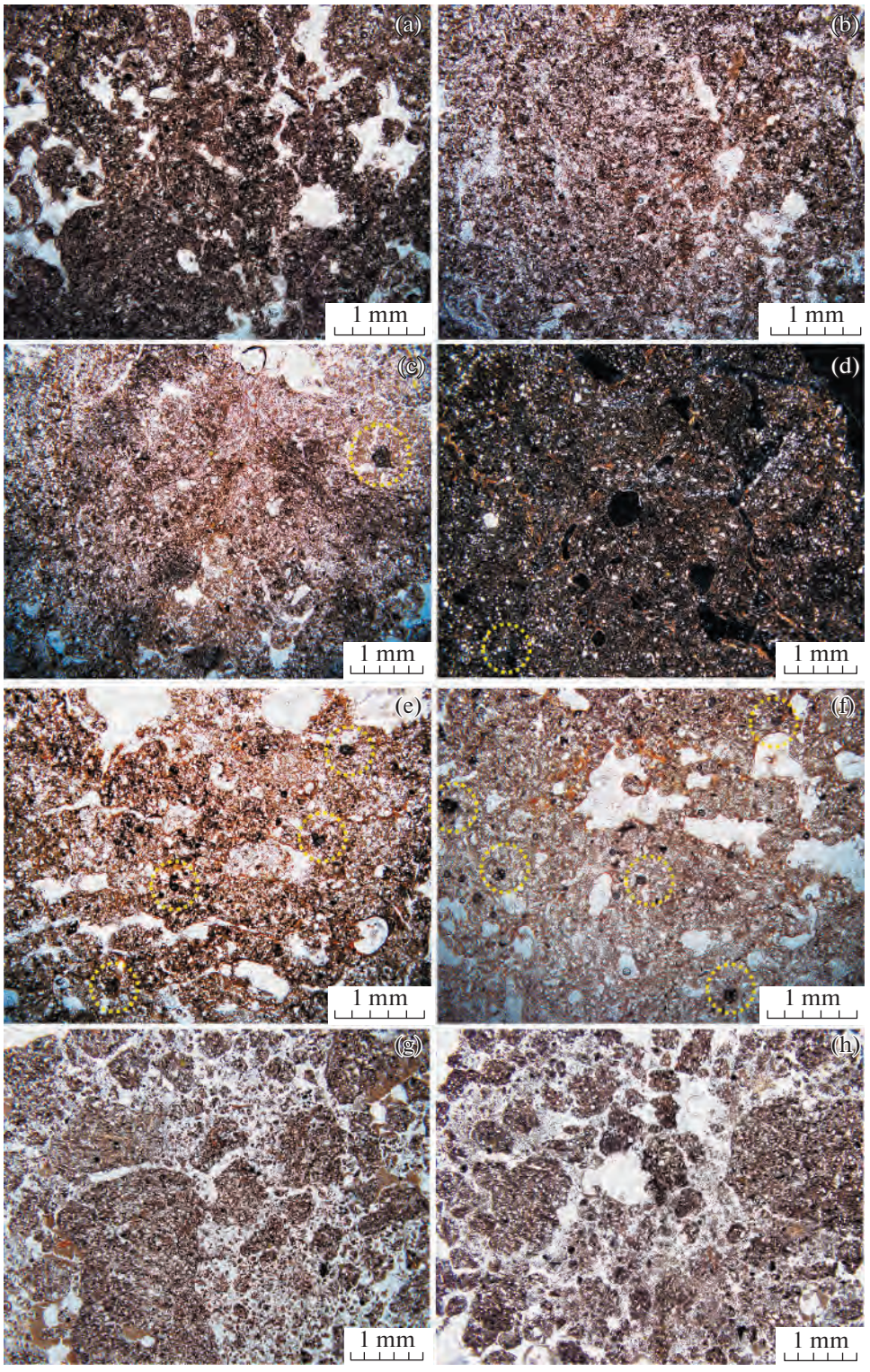

Fig. 4. Micromorphology of upper horizons. (a) – Soil 3b, 2–7 cm. Dark brown material. NII, (b) – Soil 3b, 16–24 cm. Dark brown material with rare slightly bleached microzones. NII, (c) – Soil 4b, 5–10 cm. Dark brown and brown microzones incorporation. NII, (d) – Soil 5b, 22–28 cm. Thick silty coatings within the pore space. Note abundant thin clay coatings. NX, (e) – Soil 2b, 0–10 cm. Dark brown and brown microzones incorporation. NII. Note abundant brown microzones. NII, (f) – Soil 2b, 16–24 cm. Bleached brown material with numerous clay coatings. NII, (g) – Soil 1s, 5–10 cm. Brown material. NII, (h) – Soil 1s, 22–30 cm. Thick silty coatings between brown aggregates.

On (a) and (b) note the absence of Fe-Mn pedofeatures, on (c) and (d) note few Fe-Mn micronodules (marked by yellow dashed line ellipse), on (e) and (f) note abundant Fe-Mn micronodules (marked by yellow dashed line ellipses).

Table 1. Ratios of immobile elements in the buried and the surface soils
Таблица 1. Соотношение неподвижных элементов в погребенных и фоновой почвах

Ratio	Ratio value in parent material					Arithmetic mean for soil profiles / (variation coefficients, %)				
	1s*	2b	3b	4b	BS5	1s	2b	3b	4b	5b
	100–150**	100–140	100–150	100–140	100–120	*n**** = 9	*n* = 10	*n* = 9	*n* = 8	*n* = 8
Ti/Zr	9	7	8	7	6	7/(20)	7/(3)	7/(7)	7/(8)	7/(5)
Ti/Nb	276	277	268	280	277	274 (3)	276/(4)	273/(4)	280/(4)	285/(4)
Ti/Al	0.10	0.11	0.11	0.11	0.11	0.10 (10)	0.10/(7)	0.10/(3)	0.10/(6)	0.10/(4)

* – soil profile index; ** – depth of the sampled parent strata in cm; *** – *n* – number of samples in a soil profile.

the upper and middle horizons, indicating intense leaching of these elements. However, in the surface and buried soils 2b and 4b, the absolute values of EIC in the middle horizons for Ca and Sr are higher than in buried soils 3b and 5b (fig. 7), which may indicate less humid climatic conditions that existed before the burial of the latter.

The analysis of the SiO_2/Al_2O_3 ratio showed that the studied soils have different levels of this parameter both in their upper horizons and in the parent material (fig. 8). The surface soil 1s and the buried soil 2b are remarkable for the high SiO_2/Al_2O_3 ratio in their topsoil material (fig. 8), which might be associated with losses of fine particles with infiltrating water and/or relative accumulation of quarts. The maximum value of this ratio in the subsoil is typical of the buried soil 4b, 5b and 2b (fig. 8) which more likely is associated with a lithological factor. The buried soil 3b is characterised by a low SiO_2/Al_2O_3 ratio and very smooth changes of this parameter across soil horizons, which makes it different from other soils. The enrichment of the uppermost horizons with Si in the surface soil is in agreement with sand enrichments to losses of finer material with infiltrating water while the accumulation in the lower strata can be due to the effect of underlying sandy lithology.

The study of *iron*, the element with medium mobility dependent on redox condition, helps to detect its participation in pedogenic processes. The depth functions of total iron (Fetotal) content normalised to immobile element Al revealed the absence of distinct patterns in total iron distribution throughout the soil profiles. The divergence in Fe_2O_3/Al_2O_3 values from parent material (fig. 9, (a)) does exceed 10–15% in most of the buried soils (2b, 3b and 4b). In the surface soil and the buried soil 5b the divergence is slightly higher (30%) (fig. 9, (a)). The EIC values in the surface soil are negative, indicating that Fe has been depleted in the soil strata, especially in upper horizons, while in the buried soil 5 the EIC values are positive, indicating the slight enrichment of the solum with this element, especially in the upper part of the horizons BtC. The study of iron fractions revealed that the share of pedogenic, or free, iron (Fed) of the total iron concentrations (Fetotal) is rather low, and the silicate iron compounds prevail over others (fig. 9, (b)). The proportion of pedogenic iron in total iron content indicating weathering intensity (Vodyanitsky, 2008) varies across different soils and soil horizons within a relatively narrow range from 26 to 36%. The highest share of Fed is found in the upper horizons of soil 5b (fig. 9, (b)). However, the free iron that occurs in this soil is represented mainly by non-active crystalline forms (85–95%, fig. 9, (c)). The contribution of the crystalline compounds to pedogenic iron is also high in soils 3b and 4b compared to the surface soil 1s and the buried soil 2b, where the relative proportion of crystalline iron is distinctly lower (fig. 9, (c)), and the contribution of the oxalate extractable (non-crystalline, Feo) iron to the pedogenic iron is higher. In the upper horizons of these two soils, pedogenic iron has the highest values of 26–18%, compared to similar horizons of soils 3, 4 and 5 with a very low iron activity index (Feo/Fed).

←

Рис. 4. Микроморфология верхних горизонтов. (a) – почва 3b, 2–7 см. Темно-коричневый материал. NII, (b) – почва 3b, 16–24 см. Темно-коричневый материал с немного осветленной частью. NII, (c) – почва 4b, 5–10 см. Темно-коричневый материал с коричневыми микрозонами. NII, (d) – почва 5b, 22–28 см. Мощные пылеватые кутаны в поре. Отмечены обильные тонкие глинистые кутаны. NX, (e) – почва 2b, 0–10 см. Темно-коричневый материал с коричневыми микрозонами NII, (f) – почва 2b, 16–24 см. Осветленный коричневый материал с глинистыми кутанами. NII, (g) – почва 1s, 5–10 см. Коричневый материал. NII, (h) – почва 1s, 22–30 см. Мощные пылеватые кутаны между коричневыми агрегатами.

На рисунках (a) и (b) обратите внимание на отсутствие Fe-Mn конкреций, на (c) и (d) обратите внимание на несколько Fe-Mn микроконкреций (отмечены желтым пунктирным эллипсом), на (e) и (f) обратите внимание на обильные Fe-Mn конкреции (обозначены желтыми пунктирными эллипсами).

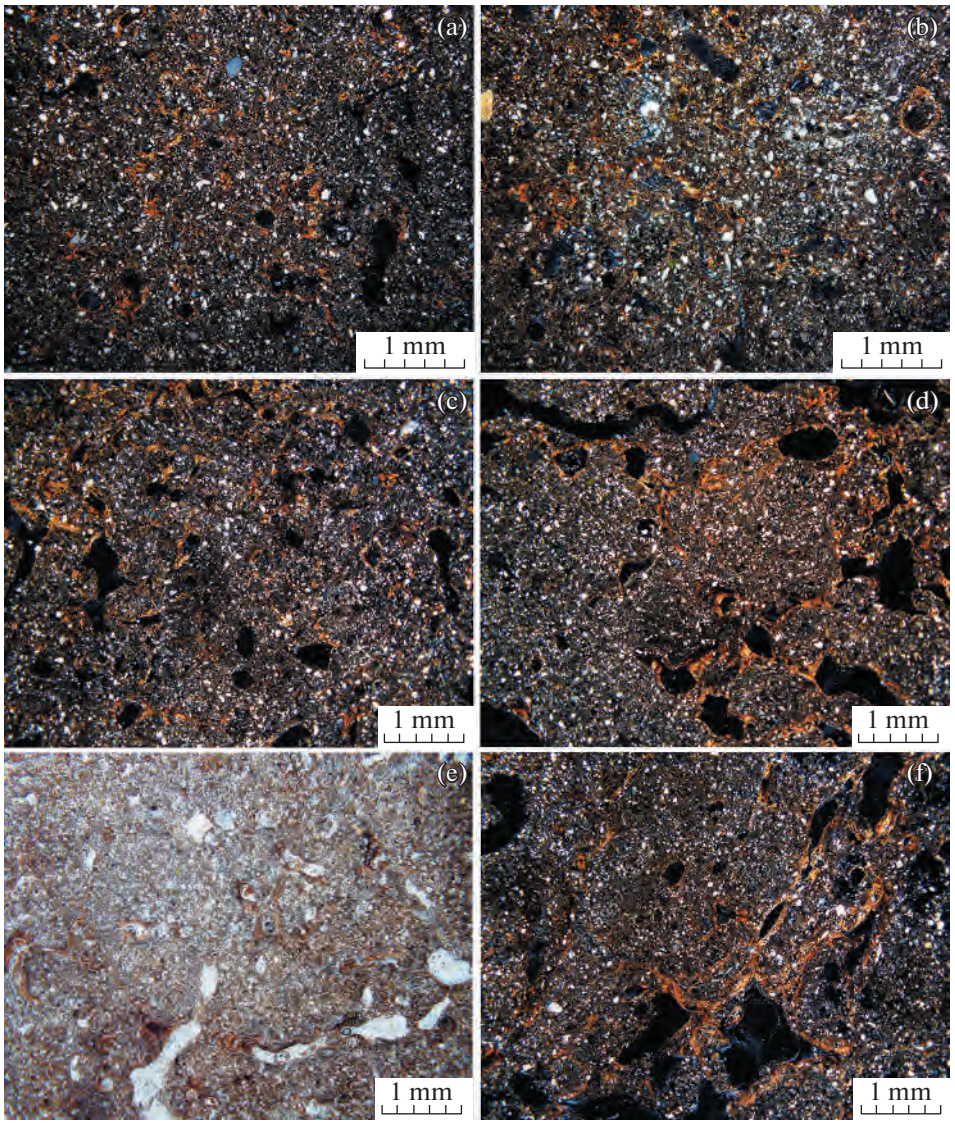

Fig. 5. Micromorphology of middle horizons. (a) – Soil 3b, 27–32 cm. Rare thin clay coatings cover about 30% of pores. NX, (b) – Soil 3b, 50–58 cm. Clay coatings cover about 60% of pores. NX, (c) – Soil 5b, 30–36 cm. Abundant clay coatings, covering 80–90% of pores. NX, (d) – Soil 4b, 50–60 cm. Thick clay coatings within the pore space cover up to 90% of pores. NX, (e) – Soil 2b, 24–30 cm. Compound clay coatings with dark brown and brown layers. NII, (f) – Soil 1s, 60–67 cm. Compound clay coatings covering 80–90% of pores. NX.

Рис. 5. Микроморфология средних горизонтов. (a) – почва 3b, 27–32 см. Тонкие глинистые кутаны покрывают ~30% пор. NX, (b) – почва 3b, 50–58 см. Глинистые кутаны покрывают 60% пор. NX, (c) – почва 5b, 30–36 см. Обильные глинистые кутаны покрывают 80–90% пор. NX, (d) – почва 4b, 50–60 см. Мощные глинистые кутаны покрывают 90% пор. NX, (e) – почва 2b, 24–30 см. Составные глинистые кутаны с темно-коричневыми и коричневыми слоями. NII, (f) – почва 1s, 60–67 см. Составные глинистые кутаны покрывают 80–90% пор. NX.

In summary, the study of the chemical composition of the five soils, one surface soil and four buried ones, implies that the surface soil 1f has many similar features with the buried soil 2b, while other soils have only partial similarity (the soil 4b and to a lesser extent soil 5b) or little similarities (soil 3b). The latter soil, in contrast to soils 1f and 2b, displays many features which might indicate drier conditions of its formation that existed before its burial (limited losses of Ca and Sr from the upper and middle soil horizons, higher share of crystalline forms in the pedogenic iron, lower values of SiO_2/Al_2O_3 ratio and their very smooth vertical changes in the profile). The soil 5b is similar to soil 3b, while the buried soil 4b occupies an intermediate position between the soils 1f and 2b, and "drier" soils 5b and especially 3b.

4.5. Pollen analysis. The sample from the surface soil (1s) turned out to be the most representative quantitatively and taxonomically diverse. The pollen spectrum more or less adequately reflects the modern veg-

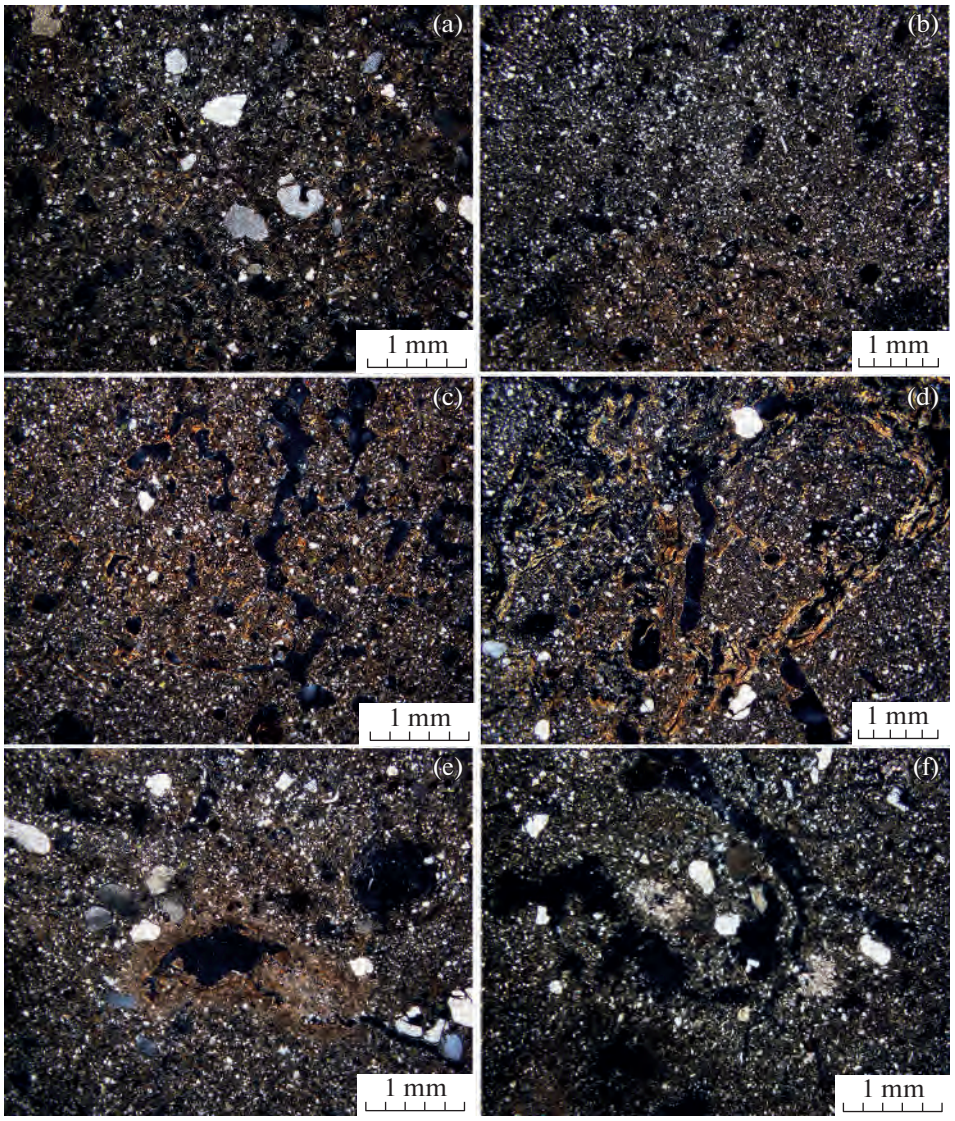

Fig. 6. Micromorphology of lower horizons. (a) – Soil 3b, 80–90 cm. Single thin clay coatings cover about 5–10% of pores. NX, (b) – Soil 4b, 90–100 cm. Rare thin clay coatings cover about 10–15% of pores. NX, (c) – Soil 2b, 84–94 cm. Clay coatings, covering 40–50% of pores. NX, (d) – Soil 1s, 90–100 cm. Thick clay coatings within the pore space cover up to 70–80% of pores. NX, (e) – Soil 3b, 115–123 cm. Complex clay-carbonate coatings with upper dark-brown clay coatings and micritic lower layer. NX, (f) – Soil 3b, 115–123 cm. Sparite nodules. NX.

Note the increasing amount of coatings from A to C.

Рис. 6. Микроморфология нижних горизонтов. (a) – почва 3b, 80–90 см. Единичные тонкие глинистые кутаны покрывают 5–10% пор. NX, (b) – почва 4b, 90–100 см. Редкие тонкие глинистые кутаны покрывают 10–15% пор. NX, (c) – почва 2b, 84–94 см. Глинистые кутаны, покрывающие 40–50% пор. NX, (d) – почва 1s, 90–100 см. Мощные кутаны в поровом пространстве, которые покрывают 70–80% пор. NX, (e) – почва 3b, 115–123 см. Комплексные глинисто-карбонатные кутаны с темно-коричневыми глинистыми кутанами сверху и микритовыми кутанами снизу. NX, (f) – почва 3b, 115–123 см. Нодули спарита. NX.

Отмечено увеличение количества и мощности кутан от горизонта A к горизонту C.

etation of the territory – a broadleaf forest (*Quercus robur*, *Tilia cordata*) with an undergrowth of *Corylus* and *Euonymus verrucosus*. At the same time, *Pinus silvestris* dominates AP group (fig. 10), accounting for up to 57% of 75.9% of AP total percentage. This feature is very characteristic of the palynospectra of the northern forest-steppe (Novenko et al. 2016) and occurs from the high pollen productivity of pine and the good adaptability of its pollen to air transport.

The group of non-arboreal pollen (24.1% in total) is dominated by pollen of Asteraceae, Chenopodiaceae, Poaceae and Cyperaceae, which is quite consistent with the geobotanical description of the territory (*Chenopodium album, Carex pilosa*) and a photo show-

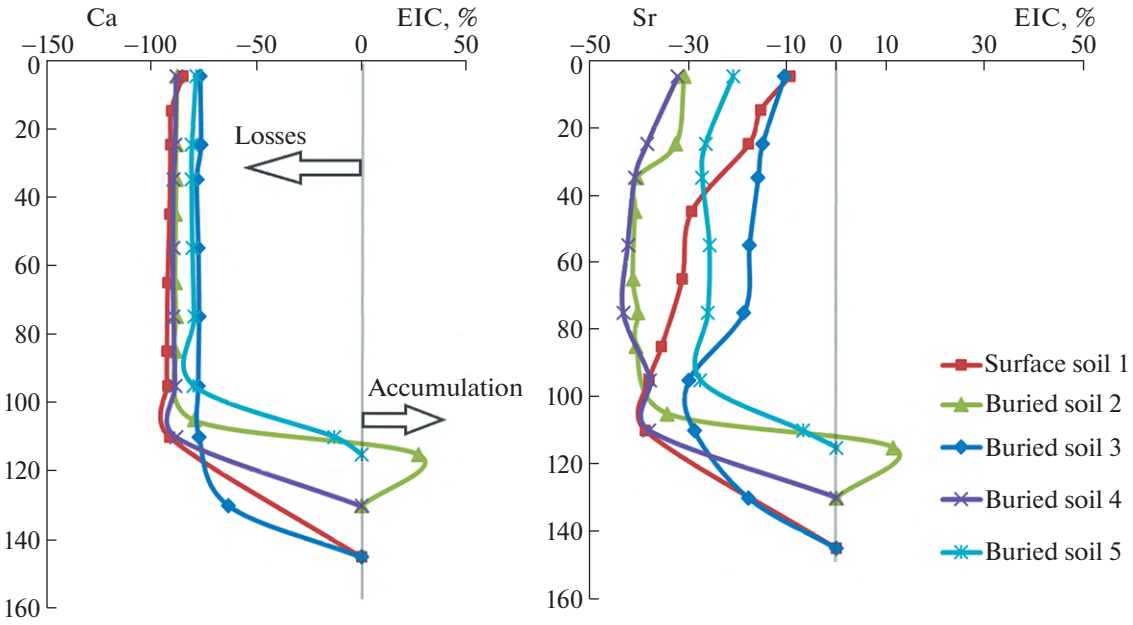

Fig. 7. Depth functions of eluvial – illuvial coefficients (EIC) calculated for CaO and Sr.
Рис. 7. Распределение элювиально-иллювиальных коэффициентов (ЭИК) по профилю, рассчитанные для CaO и Sr.

ing that arable land is adjacent to the forest. The group of synanthropic plants is represented by pollen of Urticaceae, *Plantago* sp., *Artemisia*, *Chicorium, Centaurea cyanus* and some others (see pollen diagram). In general, the composition of NAP group reflects the xerophytic appearance of herbaceous vegetation. *Sphagnum* mosses and *Lycopodium annotinum* dominate the spores group.

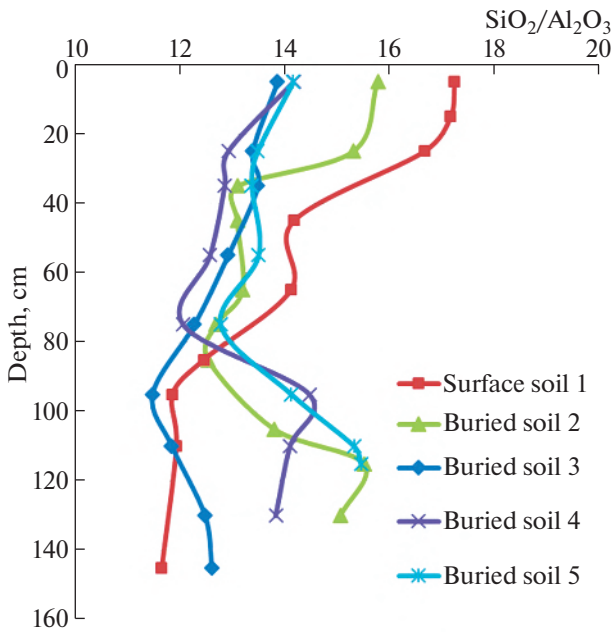

Fig. 8. Depth function of SiO_2/Al_2O_3 ratio for the surface soil 1s and the buried soils 2b, 3b, 4b, 5b.
Рис. 8. Распределение отношения SiO_2/Al_2O_3 по профилю для фоновой почвы 1s и погребенных почв 2b, 3b, 4b, 5b.

Pollen spectra from paleosols have quite significant differences both from the surface soil and from each other. An extremely small amount of Scots pine pollen in all samples from buried soils may indicate a higher productivity of plants of local biocenoses. Our data show that the common difference between the spectra from buried and surface soils is a significantly smaller proportion of arboreal pollen (from 26.1 to 49.4% versus 75.9%, respectively). The dominant in the spectra from buried soils is birch pollen, a pioneer plant of secondary forests inhabiting areas of clear cuts and conflagrations. It actively replaces pine and broadleaf plants as a much more competitive plant (Kuznetsova et al., 2019).

A large number of charcoal microparticles as well as single findings of *Gelasinospora,* an indicator of fires (van Geel, 1986) were recorded in all samples from buried soils. In the herbaceous part of the spectra, pollen from plants of arid steppes and field weeds is most abundant, which, along with the presence of pollen of *Ephedra*, Euphorbiaceae, Cannabaceae indicates a significant agro-load on landscapes and a greater heat supply and dryness of the climate. In general, the composition of the spectra is characteristic of the forest-steppe with sections of birch forests, meadow communities, and a significant proportion of ploughed territories.

Among pollen assemblage from the soil buried under the mound No. 86 and dating back to the second half of the 11th century (the 2b soil), birch pollen

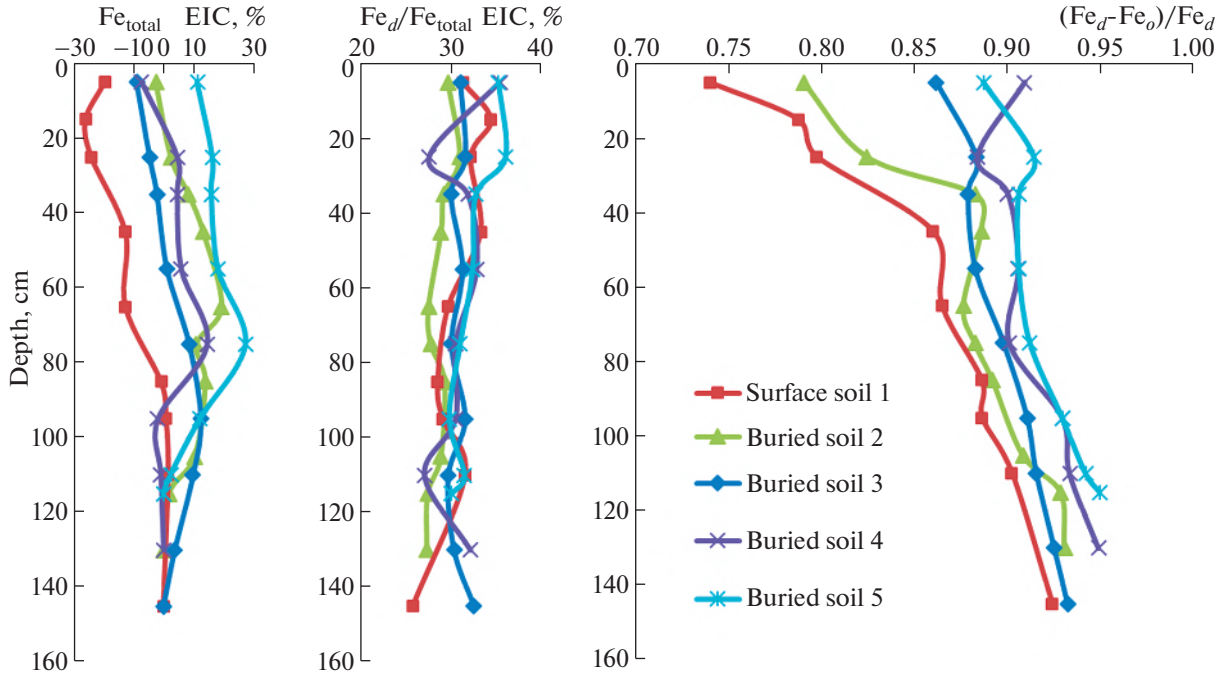

Fig. 9. Depth functions of eluvial – illuvial coefficients (EIC) calculated for total Fe (a) and weathering indexes (b, c) in the surface and the buried soils.

Рис. 9. Распределение элювиально-иллювиальных коэффициентов (ЭИК) по профилю, рассчитанных для общего железа (a) и индексов выветривания (b, c) в фоновой и погребенных почвах.

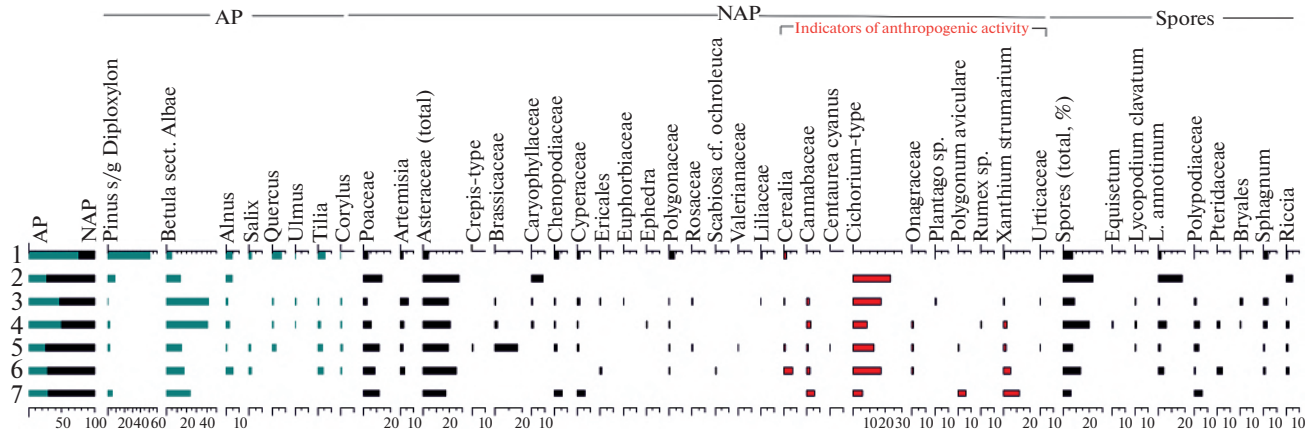

Fig. 10. Pollen diagram of the Gochevsky site: *1* – surface soil 1s, *2* – buried soil 3b, *3* – buried soil 2b (1), *4* – buried soil 2b (2), *5* – buried soil 4b, *6* – buried soil 5b (1), *7* – buried soil 5b (2).

Рис. 10. Пыльцевая диаграмма Гочевского участка: *1* – фоновая почва 1s, *2* – погребенная почва 3b, *3* – погребенная почва 2b (1), *4* – погребенная почва 2b (2), *5* – погребенная почва 4b, *6* – погребенная почва 5b (1), *7* – погребенная почва 5b (2).

dominates (more than 40%), which may indicate the presence of a birch-oak forest at the time of the burial. In the pollen spectrum from the 3b soil, the pollen of herbaceous plants accounts for more than 72%, of which almost 50% is pollen of Asteraceae and Cichorioideae. Taking into account the almost complete absence of pollen from plants typical of meadow-steppe communities, this, apparently, may reflect the wide distribution of open steppe spaces or arable land around the site of the burial mound. However, the unsatisfactory preservation of pollen indicates that a certain part of it, including pollen of herbaceous plants, has completely decomposed, and in this case any paleogeographic conclusions will be very arbitrary.

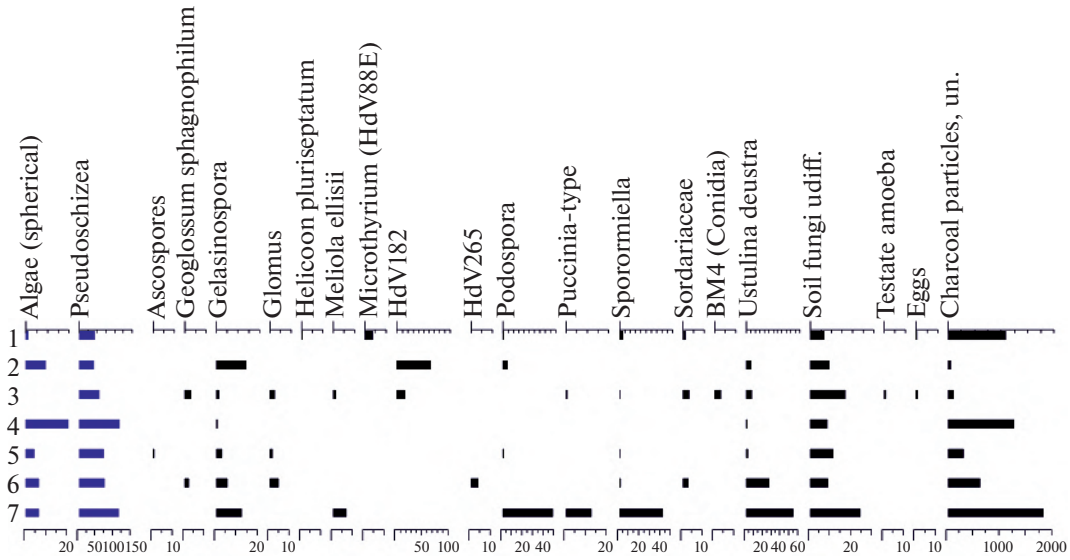

Fig. 11. NPP diagram of the Gochevsky site: *1* – surface soil 1s, *2* – buried soil 3b, *3* – buried soil 2b (1), *4* – buried soil 2b (2), *5* – buried soil 4b, *6* – buried soil 5b (1), *7* – buried soil 5b (2).

Рис. 11. Диаграмма непыльцевых палиноморф Гочевского комплекса: *1* – фоновая почва 1s, *2* – погребенная почва 3b, *3* – погребенная почва 2b (1), *4* – погребенная почва 2b (2), *5* – погребенная почва 4b, *6* – погребенная почва 5b (1), *7* – погребенная почва 5b (2).

In the 5b soil, the maximum content of Cannabaceae pollen was documented, which can be interpreted as a signal of hemp cultivation in the region, which is consistent with the pollen evidence from the Sudzha oxbow lake in the Kursk region (Shumilovskikh et al., 2019).

The NPP group is poorly diverse (fig. 11). Only soil algae *Pseudoschizea* are abundant, as well as spores of the coprophilous fungi *Sporormiella* and *Sordaria*, which may indicate the proximity of the pasture zone. The abundance of algae *Pseudoschizea* is not entirely clear and, in general, is hardly characteristic of xerophytic environments. However, soil algae are able to exist even under extremely unfavorable environmental conditions, which explains their wide distribution and the speed of their growth even with the short-term appearance of favorable factors, in the case of xerophytic conditions – during the rainfall season.

All the soils were formed in loess sediments and were classified as *Folic Greyzemic Luvic Phaeozem Cutanic*. Uncoated silt and sand grains on the ped faces in the lower part of a humic horizon (AhE) indicate greyzemic features. The argic horizon clay cutans on the ped surfaces indicate that all studied soils passed through the forest pedogenesis.

Despite the similarities, the detailed analysis of the morphological and chemical features made it possible to identify the difference between the studied soils and to relate them to climatic changes that took part in the 11th century and set a transition from a dryer period to subsequent humidification of the climate.

Our results showed that soil 3b, which was buried approximately at the beginning of the 11 century, displays many signs of drier conditions such as the darker colour of the humus horizon, less accumulation of Fe–Mn concretions and presence of sparite nodules. The results of analysis of elemental limited losses of Ca and Sr from the upper and middle soil horizons, a higher share of crystalline forms in the pedogenic iron, lower values of SiO_2/Al_2O_3 ratio and their very smooth vertical changes in the profile composition also points to drier conditions before the burial of the 3b soil. In addition, according to pollen records, the spectra of this soil are dominated by pollen of herbaceous plants, mainly Asteraceae and Cichorioideae, accounting for 72%, which reflects the existence of open spaces around the mound, most likely arable land.

The shift to a more humid environment coincided with the burial of soil 5b and 4b. Humidification of the climate increased up to the recent levels over a short period towards the burial of the soil 2b, which took place in the second half of the 11 century (fig. 12). Buried soil 2b has many properties similar to the surface soil, such as expression of greyzemic features, both soils showed a high SiO_2/Al_2O_3 ratio in their topsoil material, which also indicates wetter conditions. Pollen data from this soil indicate the presence of a birch-oak forest around the mound site.

5. CONCLUSIONS

The soils studied at the Gochevsky burial ground (including the surface soil and five buried soils under mounds) have developed over different periods but

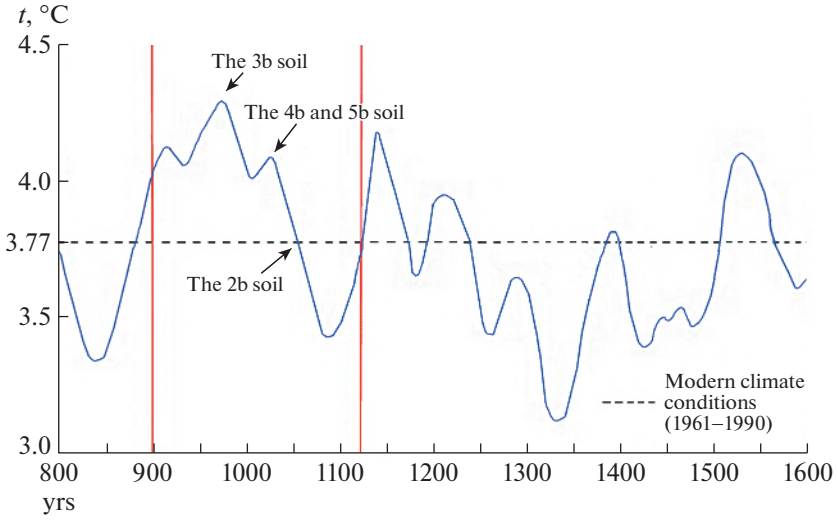

Fig. 12. Average annual air temperature in the central part of the Russian Plain in the 9th–16th centuries. The graph shows the suggested burial time of the studied soils (after Klimenko et al., 2001).

Рис. 12. Среднегодовая температура воздуха в центральной части Русской равнины в IX–XVI вв. На графике показаны предполагаемые даты погребения исследованных почв (по Клименко и др., 2001).

show relatively small differences in other soil-forming factors and, therefore can be used as a soil chronosequence to identify the differences between the present environment and the environments that existed at the time of the soil burial in the middle and the second half of the 11th century.

According to a set of soil properties, the soil can be arranged chronologically: soil 3b – 4b and 5b – soil 2b (fig. 12). Soil, which was buried approximately at the beginning of the 11 century (3b), displays signs of drier conditions. According to pollen records, the spectra of the above mentioned soils are dominated by pollen of herbaceous plants, mainly Asteraceae and Cichorioideae, accounting for 72%, which reflects the existence of open spaces around the mound.

Humidification of the climate increased to the present level in a short period towards to the soil 2b burial, which occurred in the second half of the 11th century. The transition to a more humid environment coincided with the burial of soils 5b and 4b. Pollen data from these soils indicate the presence of a birch-oak forest around the mound site.

RECONSTRUCTION OF MEDIEVAL PALEOLANDSCAPES BASED ON THE STUDY OF PALEOSOLS OF GOCHEVSKY ARCHAEOLOGICAL COMPLEX (KURSK REGION, RUSSIA)

F. G. Kurbanova[a,#], T. A. Puzanova[b], E. N. Aseyeva[b], P. G. Kust[c], and O. V. Rudenko[d]

[a] *Institute of Geography RAS, Moscow, Russia*

[b] *Lomonosov Moscow State University, Faculty of Geography, Moscow, Russia*

[c] *Dokuchaev Soil Science Institute, Moscow, Russia*

[d] *Turgenev Orel State University, Orel, Russia*

[#] *E-mail: fatima.kurbanova@igras.ru*

Due to isolation from the external environment, the soils buried under the mounds of burial complexes are valuable natural archives that provide information on the past environments. Soils buried under mounds in the Middle Ages with a short time interval – 25–50 years were studied in present paper. The research included the detailed field morphological description of the buried soils, particle size analysis and the study of elemental composition, iron fraction, some other chemical parameters and spores, pollen and non-pollen palynomorphs. Surface soil in the immediate vicinities of the mounds was studied for comparison. The data obtained allowed the forest-steppe landscape dynamics in the 11th century. Medieval warming and subsequent humidification of the climate over a short period could significantly impact natural conditions and the migration of the population of the steppes of Eurasia.

Keywords: paleosols, pollen, paleoclimate, Holocene, Medieval Climatic Optimum

ACKNOWLEDGEMENTS

The authors are grateful to Olga Khokhlova for assistance in field studies. Spore-pollen and soil analysis, micromorphological investigations and field research was financially supported by the Russian Science Foundation (project No. 19-18-00327). Analysis of iron fractions were performed in the framework of the State Task of the Institute of Geography, Russian Academy of Sciences No. AAAA-A19-119021990092-1 (FMWS-2019-0008).

REFERENCES

Beug H.J. Leitfaden der Pollenbestimmung für Mitteleuropa und angrenzende Gebiete (Guide to the Pollen Analysis for Central Europe and the Adjacent Areas). Verlag Dr. Friedrich Pfeil, München, 2004. 542 p.

Borisenkov E.P. and Pasecki V.M. Extreme natural phenomena in Russian chronicles of the XI–XVII centuries. Leningrad: Hydrometeoizdat (Publ.), 1983. 241 p. (in Russ.) Database for Palynological Data (PalDat) [Electronic data]. URL: https://www.paldat.org/

European Pollen Database [Electronic data]. URL: http://www.europeanpollendatabase.net/index.php

FAO Guidelines for soil description. Fourth edition. Rome: Food and Agriculture Organization of The United Nations, 2006. 109 p.

Goosse H., Guiot J., Mann M.E., Dubinkina S., and Sallaz-Damaz Y. The medieval climate anomaly in Europe: Comparison of the summer and annual mean signals in two reconstructions and simulations with data assimilation Global and Planetary Change. 2012. No. 84–85. P. 35–47.

Grimm E.C. TILIAGRAPH vl.25 (computer software). Illinois State Museum, Research and Collections Center, Springfield, IL, USA. 1991.

IUSS Working Group WRB. World Reference Base for Soil Resources 2014, update 2015. An international soil classification system for naming soils and creating legends for soil maps. World Soil Resources Reports 106. Rome: FAO, 2015. 203 p.

Khokhlova O.S. Short-term variability of properties of paleosols buried under Earth mounds (kurgans) and temporal scale of the derived paleoclimatic reconstructions. *Materialy Vserossiiskoi nauchnoi konferentsii, posvyashchennoi pamyati professora A.A. Velichko (Moskva, 23–25 noyabrya 2016 g.)*. Moscow, 2016. P. 591–596. (in Russ.)

Klimenko V.V., Klimanov V.A., Sirin A.A., and Sleptsov A.M. Climate changes in Western European Russia in the late Holocene. *Doklady Earth Sciences*. 2001. Vol. 377 (2). P. 190–194.

Kupriyanova L.A. and Aleshina L.A. Pollen and spores of plants of the USSR flora. Vol. 1. Leningrad: Nauka (Publ.), 1972. 171 p. (in Russ.)

Kurbanova F.G., Puzanova T.A., Rudenko O.V., and Starodubtsev G.V. Dataset on the soils of Medieval archaeological monuments in the forest-steppe zone of the East European Plain. Data in Brief. 2020. No. 30. P. 1–24.

Kuznetsova N. and Sautkina M. Forest State and Dynamics of their Species Composition in the Central Federal Distric. *Lesovedenie i lesovodstvo*. 2019. No. 2. P. 25–45. (in Russ.)

Makeev A.O., Rusakov A.V., Kurbanova F.G., Khokhlova O.S., Kust P., Lebedeva M.P., Milanovskiy E.Yu., Egli M., Denisova E., Aseyeva E.N., Rusakova E., and Mihailov E.A. Soils at archaeological monuments of the bronze age – a key to the Holocene landscape dynamics in the broadleaf forest area of the Russian Plain. *Quaternary International*. 2020. Vol. 590. P. 1–22. https://doi.org/10.1016/j.quaint.2020.09.015

Marsan F.A., Bain D.C., and Duthie D.M.L. Parent material uniformity and degree of weathering in a soil chronosequence, northwestern Italy. *Catena*. 1988. Vol. 15. No. 6. P. 507–517. https://doi.org/10.1016/0341-8162(88)90002-1

Mehra O.P. and Jackson M.L. Iron oxide removal from soils and clays by a dithionite-citrate system buffered with sodium bicarbonate. *Clays and Clay Minerals*. 1960. No. 7. P. 317–327. https://doi.org/10.1346/CCMN.1958.0070122

Muir J.W. and Logan J. Eluvial/illuvial coefficients of major elements and the corresponding losses and gains in three soil profiles. *European Journal of Soil Science*. 1982. Vol. 33. No. 2. P. 295–308. https://doi.org/10.1111/j.1365-2389.1982.tb01767.x

Munsell Soil Color Charts. Grand Rapids: Munsell Color, 2014.

Novenko E.Y., Tsyganov A.N., Rudenko O.V., Volkova E.V., Zuyganova I.S., Babeshko K.V., Olchev A.V., Losbenev N.I., Payne R.J., and Y.A. Mazei. Mid- and late-Holocene vegetation history, climate and human impact in the forest-steppe ecotone of European Russia: new data and a regional synthesis. *Biodiversity and Conservation*. 2016. Vol. 25. No. 12. P. 2453–2472. https://doi.org/10.1007/s10531-016-1051-8

Puzanova T.A., Aseeva E.N., Lebedeva M.P., Kurbanova F.G., and Chernov T.I. The methods of re-search of buried soils under archaeological sites. Proceedings of 18 international multidisciplinary scientific geoconference SGEM 2018, Soils, Forest ecosystems, Marine and Ocean Ecosystems, Sofia, Bulgaria. 2018. Vol. 16. P. 611–619. http://dx.doi.org/10.5593/sgem2018/3.2

Schaetzl R.J. and Anderson S. Soils: Genesis and Geomorphology. New York: Cambridge University Press, 2005. 833 p.

Sheldon N.D. and Tabor N.J. Quantitative paleoenvironmental and paleoclimatic reconstruction using paleosols'. *Earth-Science Reviews*. 2009. Vol. 95. No. 1–2. P. 1–52. https://doi.org/10.1016/j.earscirev.2009.03.004

Shoba S.A. (Ed.) *Natsional'nyi atlas pochv Rossiiskoi Federatsii* (National Soil Atlas of Russian Federation). Moscow: Astrel (Publ.), 2011. 632 p. (in Russ.)

Shumilovskikh L.S., Rodinkova V.Ye., Rodionova A., Troshina A., Ershova E., Novenko E., Zazovskaya E., Sycheva S.A., Kiselev D.I., Schlütz F., and Schneeweiß J. Insights into the late Holocene vegetation history of the East European forest-steppe: case study Sudzha (Kursk

region, Russia). *Vegetation History and Archaeobotany*. 2019. No. 28. P. 513–528. https://doi.org/10.1007/s00334-018-00711-4

Shumilovskikh L.S., Shumilovskikh E.S., Schlütz F., and van Geel B. NPP-ID: Non-Pollen Palynomorph Image Database as a research and educational platform. Vegetation History and Archaeobotany. 2021. Published online. https://doi.org/10.1007/s00334-021-00849-8

Stoops G. Guidelines for Analysis and Description of Soil and Regolith Thin Sections. Madison: Soil Science Society of America, 2003. 256 p.

Targulian V.O. and Goryachkin S.V. (Eds.) Soil Memory: Soil as a Memory of Biosphere-Geosphere-Anthroposphere Interaction. Moscow: URSS (Publ.), 2008. 692 p. (in Russ.)

van Geel B. Application of fungal and algal remains and other microfossils in palynological analysis. *Handbook of Holocene Palaeoecology and Palaeohydrology*. Wiley, Chichester, 1986. P. 497–505.

Vodyanitsky Y.N. Heavy metals and metalloids in soils. Moscow: Dokuchaev Soil Science Institute (Publ.), 2008. 86 p. (in Russ.)